Article

Radical Coupling Reaction of Paramagnetic Endohedral Metallofullerene La@C

Yuta Takano, Akinori Yomogida, Hidefumi Nikawa, Michio Yamada, Takatsugu Wakahara, Takahiro Tsuchiya, Midori O. Ishitsuka, Yutaka Maeda, Takeshi Akasaka, Tatsuhisa Kato, Zdenek Slanina, Naomi Mizorogi, and Shigeru Nagase

J. Am. Chem. Soc., **2008**, 130 (48), 16224-16230 • DOI: 10.1021/ja802748q • Publication Date (Web): 08 November 2008

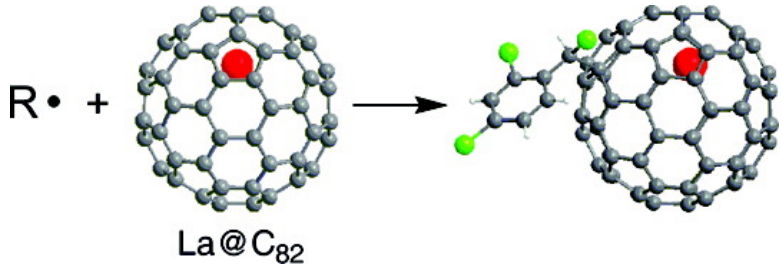

More About This Article

Additional resources and features associated with this article are available within the HTML version:

- Supporting Information
- Access to high resolution figures
- Links to articles and content related to this article
- Copyright permission to reproduce figures and/or text from this article

View the Full Text HTML

J|A|C|S
ARTICLES

Published on Web 11/08/2008

Radical Coupling Reaction of Paramagnetic Endohedral Metallofullerene La@C_{82}

Yuta Takano,[†] Akinori Yomogida,[†] Hidefumi Nikawa,[†] Michio Yamada,[†] Takatsugu Wakahara,[†] Takahiro Tsuchiya,[†] Midori O. Ishitsuka,[†] Yutaka Maeda,[‡] Takeshi Akasaka,*[,†] Tatsuhisa Kato,[§] Zdenek Slanina,[†] Naomi Mizorogi,[||] and Shigeru Nagase*[,||]

Center for Tsukuba Advanced Research Alliance, University of Tsukuba, Tsukuba, Ibaraki 305-8577, Japan, Department of Chemistry, Tokyo Gakugei University, Koganei, Tokyo 184-8501, Japan, Department of Chemistry, Josai University, Sakado, Saitama 350-0295, Japan, and Department of Theoretical and Computational Molecular Science, Institute for Molecular Science, Okazaki, Aichi 444-8585, Japan

Received April 15, 2008; E-mail: akasaka@tara.tsukuba.ac.jp; nagase@ims.ac.jp

Abstract: The thermal reaction of La@C_{82}(C_{2v}) with 3-triphenylmethyl-5-oxazolidinone (**1**) in toluene affords benzyl monoadducts La@C_{82}(C_{2v})($CH_2C_6H_5$) (**2a**−**2d**). The same monoadducts are also obtained by the photoirradiation of La@C_{82}(C_{2v}) in toluene without the existence of **1**. These reactions are applicable to paramagnetic metallofullerenes, such as La@C_{82}(C_s) and Ce@C_{82}(C_{2v}). The photoirradiation of La@C_{82}(C_{2v}) in 1,2-dichlorobenzene in the presence of α,α,2,4-tetrachlorotoluene also affords the monoadducts La@C_{82}(C_{2v})($CHClC_6H_3Cl_2$) (**3a**−**3d**). The monoadducts are fully characterized by spectroscopic analyses. Single-crystal X-ray structure analysis for **3d** reveals the unique structure. Theoretical calculations show that the cage carbons having high spin densities are selectively attacked by radical species to form the monoadducts linked by a carbon−carbon single bond. The thermal reaction of La@C_{82}(C_{2v}) with **1** in benzene affords metallofulleropyrrolidine La@C_{82}(C_{2v})($C_2H_4NCPh_3$) (**5**), unlike the reaction in toluene.

Introduction

Endohedral metallofullerenes (EMFs) are known as very promising materials in the fields of chemistry, physics, bioscience, and nanoscience.[1−5] Among many kinds of EMFs, M@C_{82} (M = group 2 and 3 metals) is most abundantly produced.[3,6] It is well-known that M@C_{82} has electronic states described by $[M]^{2+}[C_{82}]^{2-}$ and $[M]^{3+}[C_{82}]^{3-}$ because of electron transfer from the M atom onto the C_{82} cage.[7,8] As in the case of La@C_{82}, the latter electronic state leads to an open-shell electronic structure on C_{82},[8] with an unpaired electron being widely delocalized on the surface of the C_{82} cage.

Meanwhile, toluene is frequently used as a representative solvent,[2] because most fullerenes are highly soluble in toluene.

[†] University of Tsukuba.
[‡] Tokyo Gakugei University.
[§] Josai University.
[||] Institute for Molecular Science.

(1) Bethune, D. S.; Johnson, R. D.; Salem, J. R.; Devries, M. S.; Yannoni, C. S. *Nature* **1993**, *366*, 123–128.
(2) *The Chemistry of Fullerenes*; Taylor, R.; Ed.; World Scientific: Farrer, Singapore, 1995.
(3) *Endofullerenes: A New Family of Carbon Cluster*; Akasaka, T., Nagase, S., Eds.; Kluwer: Dordrecht, The Netherlands, 2002.
(4) (a) Thrash, T. P.; Cagle, D. W.; Alford, J. M.; Wright, K.; Ehrhardt, G. J.; Mirzadeh, S.; Wilson, L. *J. Chem. Phys. Lett.* **1999**, *308*, 329–336. (b) Mikawa, M.; Kato, H.; Okumura, M.; Narazaki, M.; Kanazawa, Y.; Miwa, N.; Shinohara, H. *Bioconjugate Chem.* **2001**, *12*, 510–514. (c) Kato, H.; Kanazawa, Y.; Okumura, M.; Taninaka, A.; Yokokawa, T.; Shinohara, H. *Acad. Radiol.* **2002**, *9*, S495–S497. (d) Bolskar, R. D.; Benedetto, A. F.; Husebo, L. O.; Price, R. E.; Jackson, E. F.; Wallace, S.; Wilson, L. J.; Alford, J. M. *J. Am. Chem. Soc.* **2003**, *125*, 5471–5478. (e) Okumura, M.; Mikawa, M.; Yokokawa, T.; Kanazawa, Y.; Kato, H.; Shinohara, H. *J. Am. Chem. Soc.* **2003**, *125*, 4391–4397. (f) Sitharaman, B.; Bolskar, R. D.; Rusakova, I.; Wilson, L. J. *Nano Lett.* **2004**, *4*, 2373–2378. (g) Tóth, E.; Bolskar, R. D.; Borel, A.; González, G.; Helm, L.; Merbach, A. E.; Shitaraman, B.; Wilson, L. J. *J. Am. Chem. Soc.* **2005**, *127*, 799–805. (h) Yanagi, K.; Okubo, S.; Okazaki, T.; Kataura, H. *Chem. Phys. Lett.* **2007**, *435*, 306–310. (i) Zhang, E. Y.; Shu, C. Y.; Feng, L.; Wang, C. R. *J. Phys. Chem. B* **2007**, *111*, 14223–14226.
(5) (a) Huang, H. J.; Yang, S. H. *J. Organomet. Chem.* **2000**, *599*, 42–48. (b) Yang, S. F.; Yang, S. H. *J. Phys. Chem. B* **2001**, *105*, 9406–9412. (c) Nakashima, N.; Sakai, M.; Murakami, H.; Sagara, T.; Wakahara, T.; Akasaka, T. *J. Phys. Chem. B* **2002**, *106*, 3523–3525. (d) Li, X. G.; Yang, S. F.; Yang, S. H.; Xu, Y.; Liu, Y. Q.; Zhu, D. B. *Thin Solid Films* **2002**, *413*, 231–236. (e) Yang, S. F.; Fan, L. Z.; Yang, S. H. *J. Phys. Chem. B* **2003**, *107*, 8403–8411. (f) Yang, S.; Fan, L.; Yang, S. *J. Phys. Chem. B* **2004**, *108*, 4394–4404. (g) Yasutake, Y.; Shi, Z.; Okazaki, T.; Shinohara, H.; Majima, Y. *Nano Lett.* **2005**, *5*, 1057–1060. (h) Yumura, T.; Sato, Y.; Suenaga, K.; Urita, K.; Iijima, S. *Nano Lett.* **2006**, *6*, 1389–1395. (i) Tsuchiya, T.; Sato, K.; Kurihara, H.; Wakahara, T.; Maeda, Y.; Akasaka, T.; Ohkubo, K.; Fukuzumi, S.; Kato, T.; Nagase, S. *J. Am. Chem. Soc.* **2006**, *128*, 14418–14419. (j) Tang, J.; Xing, G.; Zhao, Y.; Jing, L.; Yuan, H.; Zhao, F.; Gao, X.; Qian, H.; Su, R.; Ibrahim, K.; Chu, W.; Zhang, L.; Tanigaki, K. *J. Phys. Chem. B* **2007**, *111*, 11929–11934. (k) Perez-Jimenez, A. J. *J. Phys. Chem. C* **2007**, *111*, 17640–17645. (l) Tsuchiya, T.; et al. *J. Am. Chem. Soc.* **2008**, *130*, 450–451.
(6) (a) Johnson, R. D.; de Vries, M. S.; Salem, J.; Bethune, D. S.; Yannoni, C. S. *Nature* **1992**, *355*, 239–240. (b) Shinohara, H.; Sato, H.; Saito, Y.; Ohkouchi, M.; Ando, Y. *J. Phys. Chem.* **1992**, *96*, 3571–3573. (c) Suzuki, T.; Maruyama, Y.; Kato, T.; Kikuchi, K.; Achiba, Y. *J. Am. Chem. Soc.* **1993**, *115*, 11006.
(7) (a) Weaver, K. H.; Chai, Y.; Kroll, G. H.; Jin, C.; Ohno, T. R.; Haufler, R. E.; Guo, T.; Alford, J. M.; Conceicao, J.; Chibante, L. P. F.; Jain, A.; Palmer, G.; Smalley, R. E. *Chem. Phys. Lett.* **1992**, *190*, 460–464. (b) Hino, S.; Takahashi, H.; Iwasaki, K.; Matsumoto, K.; Miyazaki, T.; Hasegawa, S.; Kikuchi, K.; Achiba, Y. *Phys. Rev. Lett.* **1992**, *71*, 4261–4263.

10.1021/ja802748q CCC: $40.75

In this context, there is an open question why ESR signals of paramagnetic EMFs such as La@C_{82} disappear when they are stored in toluene for a long period.[3] Shinohara et al. reported that the intensity of ESR signals of La@C_{76} and La@C_{80} decreases upon the storage in toluene for a few days.[9] Interestingly, Okubo and co-workers found that the signals remain even after the one-month storage in chlorobenzene.[10]

Recently, a variety of reactions developed for fullerenes have been applied to EMFs.[11−16] Among these, radical reactions are interesting. Hence, several radical reactions of M@C_{82} have been reported.[16] Tumanskii and co-workers reported the addition of phosphoryl radicals to La@C_{82},[16a] with the adducts being obtained as a mixture of several isomers. Multiple addition of phenyl radicals to La@C_{82}, which leads to La@$C_{82}(Ph)_n$ (n = 1, 2, 3, 4, ...), was reported by Kalina and co-workers.[16b] Shinohara et al. reported that seven isomers of La@$C_{82}(C_s)$-$(C_8F_{17})_2$ were obtained by photoirradiation in the presence of perfluorooctyl iodide.[16c] Generally, free radical reactions show a low selectivity in the formation of monoadducts because of the high reactivity. To the best of our knowledge, therefore, no report is available for structural determination of monoadducts formed by radical reactions of EMFs.

Here, we present the first synthesis and isolation of monoadducts by the radical reaction of La@$C_{82}(C_{2v})$ (denoted simply as La@C_{82} hereafter). Four isomers of benzyl adducts, La@$C_{82}(CH_2C_6H_5)$ (**2a**−**2d**), are synthesized with toluene in the presence of 3-triphenylmethyl-5-oxazolidinone (**1**) and characterized. It is demonstrated that toluene shows a high reactivity to the paramagnetic La@C_{82} upon irradiation or even in sunlight. X-ray diffraction (XRD) analysis is performed for La@$C_{82}(CHClC_6H_3Cl_2)$ (**3d**). Selectivity is examined by DFT calculations. Metallofulleropyrrolidine La@$C_{82}(C_2H_4NCPh_3)$ (**5**) is also synthesized using benzene instead of toluene by the thermal reaction of La@C_{82} with **1**.

Experimental Section

General. All chemicals and solvents were obtained from Wako and Aldrich, and were used without further purification unless otherwise stated. Toluene was distilled over benzophenone sodium ketyl under an argon atmosphere prior to use in a reaction. 1,2-Dichlorobenzene (ODCB) was distilled over P_2O_5 under vacuum prior to use.

High performance liquid chromatography (HPLC) isolation was performed on an LC-908 (Japan Analytical Industry Co., Ltd.) by monitoring UV absorption at 330 nm. Toluene was used as the eluent. Mass spectrometry was performed on a Bruker BIFLEX III using 1,1,4,4-tetraphenyl-1,3-butadiene as matrix. Absorption spectra were measured using a SHIMADZU UV-3150 spectrophotometer. The ^{1}H and ^{13}C NMR measurements were carried out on a Bruker AVANCE500 with a CryoProbe system. Cyclic voltammograms (CV) and differential pulse voltammograms (DPV) were recorded on a BAS CV50W electrochemical analyzer. Platinum wires were used as the working and counter electrodes. The reference electrode was a saturated calomel reference electrode (SCE) filled with 0.1 M (n-Bu)$_4$NPF$_6$ in ODCB. CV: scan rate, 20 mV/s. DPV: pulse amplitude, 50 mV; pulse width, 50 ms; pulse period, 200 ms; scan rate, 20 mV/s.

Synthesis of Benzyl Derivatives of La@C_{82} (2a−2d). La@C_{82} was prepared and isolated as reported previously.[17] 3-Triphenylmethyl-5-oxazolidinone (**1**) was synthesized and purified as reported in the literature.[18] **1** (3.0 mg, 9.0×10^{-6} mol) was added to 50 mL of 1.2×10^{-4} M La@C_{82} (6.7 mg, 6.0×10^{-6} mol) toluene solution. The solution was refluxed under an argon atmosphere, and the reaction proceeded smoothly for 2 h. The four isomers of La@$C_{82}(CH_2C_6H_5)$ (**2a**−**d**) were isolated from the unreacted starting materials and multiadducts, by multistep HPLC as shown in Figure 1.

(8) (a) Lassonen, K.; Andreoni, W.; Parrinello, M. *Science* **1992**, *258*, 1916–1918. (b) Nagase, S.; Kobayashi, K. *Chem. Phys. Lett.* **1993**, *214*, 57–63. (c) Nagase, S.; Kobayashi, K. *Chem. Phys. Lett.* **1994**, *228*, 106–110. (d) Nagase, S.; Kobayashi, K. *J. Chem. Soc., Chem. Commun.* **1994**, 1837–1838. (e) Poirier, D. M.; Knupfer, M.; Weaver, J. H.; Andreoni, W.; Lassonen, K.; Parrinello, M.; Bethune, D. S.; Kikuchi, K.; Achiba, Y. *Phys. Rev. B* **1994**, *49*, 17403–17412.

(9) Bandow, S.; Kitagawa, H.; Mitani, T.; Inokuchi, H.; Saito, Y.; Yamaguchi, H.; Hayashi, N.; Sato, H.; Shinohara, H. *J. Phys. Chem.* **1992**, *96*, 9609–9611.

(10) Okubo, S.; Kato, T.; Inakuma, M.; Shinohara, H. *New Diamond Front. Carbon Technol.* **2001**, *11*, 285–294.

(11) For the Diels-Alder reactions, see: (a) Iezzi, E. B.; Duchamp, J. C.; Harich, K.; Glass, T. E.; Lee, H. M.; Olmstead, M. M.; Balch, A. L.; Dorn, H. C. *J. Am. Chem. Soc.* **2002**, *124*, 524–525. (b) Lee, H. M.; Olmstead, M. M.; Iezzi, E.; Duchamp, J. C.; Dorn, H. C.; Balch, A. L. *J. Am. Chem. Soc.* **2002**, *124*, 3494–3495.

(12) For the Prato reactions, see: (a) Cao, B.; Wakahara, T.; Maeda, Y.; Han, A.; Akasaka, T.; Kato, T.; Kobayashi, K.; Nagase, S. *Chem.—Eur. J.* **2004**, *10*, 716–720. (b) Lu, X.; He, G.; Feng, L.; Shi, Z.; Gu, Z. *Tetrahedron* **2004**, *60*, 3713–3716. (c) Cardona, C. M.; Kitaygorodskiy, A.; Ortiz, A.; Herranz, M. A.; Echegoyen, L. *J. Org. Chem.* **2005**, *70*, 5092–5097. (d) Cardona, C. M.; Kitaygorodskiy, A.; Echegoyen, L. *J. Am. Chem. Soc.* **2005**, *127*, 10448–10453. (e) Yamada, M.; Nakahodo, T.; Wakahara, T.; Tsuchiya, T.; Maeda, Y.; Akasaka, T.; Yoza, K.; Horn, E.; Mizorogi, N.; Nagase, S. *J. Am. Chem.* **2006**, *128*, 1402–1403.

(13) For the Bingel reactions, see: (a) Feng, L.; Nakahodo, T.; Wakahara, T.; Tsuchiya, T.; Maeda, Y.; Akasaka, T.; Kato, T.; Horn, E.; Yoza, K.; Mizorogi, N.; Nagase, S. *J. Am. Chem. Soc.* **2005**, *127*, 17136–17137. (b) Feng, L.; Wakahara, T.; Nakahodo, T.; Tsuchiya, T.; Piao, Q.; Maeda, Y.; Lian, Y.; Akasaka, T.; Horn, E.; Yoza, K.; Kato, T.; Mizorogi, N.; Nagase, S. *Chem.—Eur. J.* **2006**, *12*, 5578–5586. (c) Feng, L.; Wakahara, T.; Tsuchiya, T.; Nakahodo, T.; Piao, Q.; Maeda, Y.; Akasaka, T.; Kato, T.; Yoza, K.; Horn, E.; Mizorogi, N.; Nagase, S. *J. Am. Chem. Soc.* **2006**, *128*, 5990–5991.

(14) For the carbene addition reactions, see: (a) Maeda, Y.; et al. *J. Am. Chem. Soc.* **2004**, *126*, 6858–6859. (b) Matsunaga, Y.; Maeda, Y.; Wakahara, T.; Tsuchiya, T.; Ishitsuka, M. O.; Akasaka, T.; Mizorogi, N.; Kobayashi, K.; Nagase, S.; Kadish, K. M. *ITE Lett.* **2006**, *7*, C1. (c) Akasaka, T.; Kono, T.; Matsunaga, Y.; Wakahara, T.; Nakahodo, T.; Ishitsuka, M. O.; Maeda, Y.; Tsuchiya, T.; Kato, T.; Liu, M. T. H.; Mizorogi, N.; Slanina, Z.; Nagase, S. *J. Phys. Chem. A* **2008**, *112*, 1294–1297.

(15) For other reactions of M@C_{82}, see: (a) Akasaka, T.; Kato, T.; Kobayashi, K.; Nagase, S.; Yamamoto, K.; Funasaka, H.; Takahashi, T. *Nature* **1995**, *374*, 600–601. (b) Akasaka, T.; Nagase, S.; Kobayashi, K.; Suzuki, T.; Kato, T.; Yamamoto, K.; Funasaka, H.; Takahashi, T. *J. Chem. Soc., Chem. Commun.* **1995**, 1343–1344. (c) Suzuki, T.; Maruyama, Y.; Kato, T.; Akasaka, T.; Kobayashi, K.; Nagase, S.; Yamamoto, K.; Funasaka, H.; Takahashi, T. *J. Am. Chem. Soc.* **1995**, *117*, 9606–9607. (d) Feng, L.; Zhang, X.; Yu, Z.; Wang, J.; Gu, Z. *Chem. Mater.* **2002**, *14*, 4021–4022. (e) Lu, X.; Xu, J.; He, X.; Shi, Z.; Gu, Z. *Chem. Mater.* **2004**, *16*, 953–955. (f) Kareev, I. E.; Lebedkin, S. F.; Bubnov, V. P.; Yagubskii, E. B.; Ioffe, I. N.; Khavrel, P. A.; Kuvychko, I. V.; Strauss, S. H.; Boltalina, O. V. *Angew. Chem.* **2005**, *117*, 1880–1883. (g) Kareev, I. E.; Lebedkin, S. F.; Bubnov, V. P.; Yagubskii, E. B.; Ioffe, I. N.; Khavrel, P. A.; Kuvychko, I. V.; Strauss, S. H.; Boltalina, O. V. *Angew. Chem., Int. Ed.* **2005**, *44*, 1846–1849. (h) Yamada, M.; Feng, L.; Wakahara, T.; Tsuchiya, T.; Maeda, Y.; Lian, Y.; Kako, M.; Akasaka, T.; Kato, T.; Kobayashi, K.; Nagase, S. *J. Phys. Chem. B* **2005**, *109*, 6049–6051. (i) Li, X.; Fan, L.; Liu, D.; Sung, H. H. Y.; Williams, I. D.; Yang, S.; Tan, K.; Lu, X. *J. Am. Chem. Soc.* **2007**, *129*, 10636–10637.

(16) For radical reactions, see: (a) Tumanskii, B. L.; Bashilov, V. V.; Solodovnilov, S. P.; Sokolov, V. I. *Fuller. Sci. Technol.* **1998**, *6*, 445–448. (b) Tumanskii, B. L., Kalina, O. G., Eds. *Endofullerenes: Radical Reaction of Fullerene Derivatives*; Kluwer Academic Publishers: Dordrecht, The Netherlands, 2001; Chapter 10. (c) Tumanskii, B. L.; Tagmatarchis, N.; Taninaka, A.; Shinohara, H. *Chem. Phys. Lett.* **2002**, *355*, 226–232.

(17) (a) Yamamoto, K.; Funasaka, H.; Takahashi, T.; Akasaka, T.; Suzuki, T.; Maruyama, Y. *J. Phys. Chem.* **1994**, *98*, 2008–2011. (b) Yamamoto, K.; Funasaka, H.; Takahashi, T.; Akasaka, T. *J. Phys. Chem.* **1994**, *98*, 12831–12833.

(18) Tsuge, O.; Kanemasa, S.; Ohe, M.; Takenaka, S. *Bull. Chem. Soc. Jpn.* **1987**, *60*, 4079–4089.

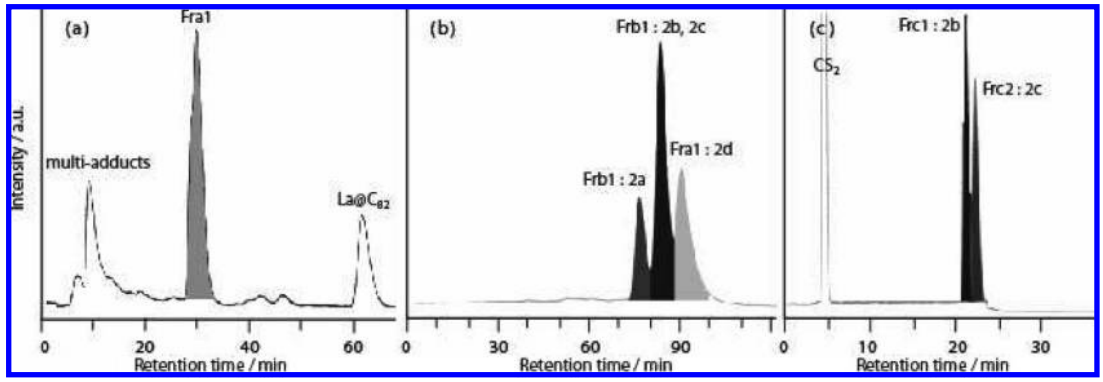

Figure 1. HPLC separation/isolation scheme for **2a**−**2d**. (a) First-stage HPLC chromatogram on a Buckyprep column (i.d. 20 mm × 250 mm), (b) second-stage HPLC chromatogram on a 5PBB column (i.d. 20 mm × 250 mm), (c) third-stage HPLC chromatogram on a Buckyprep column (i.d. 20 mm × 250 mm); eluent, toluene; flow rate, 9.9 mL/min; wavelength, 330 nm; room temperature.

La@C_{82}($CH_2C_6H_5$) (2a). Vis-near-IR (CS_2): λ_{max} = 504, 743, 820, 987, 1234, 1453 nm. MALDI-TOF MS *m/z*: calcd for $LaC_{89}H_7$ ($[M]^-$), 1213.96; found, 1214.5.

La@C_{82}($CH_2C_6H_5$) (2b). Vis-near-IR (CS_2): λ_{max} = 590, 786, 1129, 1314 nm. ^{1}H NMR (500 MHz, CS_2/CD_2Cl_2 = 3/1): δ 7.84 (d, 2H, J = 7.1 Hz), 7.47 (dd, 2H, J = 7.1, 7.4 Hz), 7.42 (t, 1H, J = 7.4 Hz), 4.82 ppm (AB quartet, 2H, Δ_{ab} = 52.5 Hz, J_{ab} =12.5 Hz). ^{13}C NMR (125 MHz, CS_2/CD_2Cl_2 = 3/1): δ 184.0, 173.4, 168.8, 158.9, 151.8, 149.5, 148.7, 148.7, 148.1, 147.9, 147.8, 147.8, 147.3, 147.0, 146.9, 146.6, 146.2, 146.1, 146.0 (2C), 145.6 (2C), 144.7, 144.6, 144.5, 144.1, 143.9 (2C), 143.7, 143.3, 142.9, 142.5, 142.4, 142.1 (2C), 142.0, 141.6, 141.6, 141.4, 140.9, 140.6, 140.5, 140.2, 139.8, 139.4, 139.3 (2C), 139.0, 138.8, 138.5, 138.4, 138.4, 138.1, 137.5, 137.5, 137.4, 137.2, 137.1, 136.6 (2C), 136.1, 136.0, 135.8 (2C), 135.63 135.5, 135.4 (Ph), 135.3, 135.2, 135.0, 134.7, 134.1, 134.0, 133.8, 133.7, 133.4, 133.3, 133.1, 132.0, 131.2, 131.1 (Ph), 130.1, 129.8, 128.1 (Ph), 127.6 (Ph), 62.2 (fullerenyl sp^3 carbon), 47.7 ppm (CH_2). MALDI-TOF MS *m/z*: calcd for $LaC_{89}H_7$ ($[M]^-$), 1213.96; found, 1214.5.

La@C_{82}($CH_2C_6H_5$) (2c). Vis-near-IR (CS_2): λ_{max} = 566, 984, 1401 nm. ^{1}H NMR (500 MHz, CS_2/CD_2Cl_2 = 3/1): δ 7.32−7.29 (m, 2H), 7.28−7.23 (m, 2H), 7.25−7.24 (m, 1H), 3.61 ppm (AB quartet, 2H, Δ_{ab} = 15.5 Hz, J_{ab} = 2.1). ^{13}C NMR (125 MHz, CS_2/CD_2Cl_2 = 3/1): δ 173.7, 168.0, 165.0, 159.7, 155.6, 154.6, 153.9, 153.7, 152.1, 151.3, 151.0, 150.8, 149.3, 148.3, 147.9, 147.9, 147.3, 146.9, 146.6, 146.3, 146.2, 146.2, 145.9 (2C), 145.3, 145.2, 145.1, 145.0, 144.8, 144.6, 144.4, 144.0, 143.9, 143.8 (2C), 143.7, 143.0, 142.8, 142.2, 141.7, 141.0, 140.8, 140.5, 139.8 (2C), 139.6, 139.5 (3C), 139.1, 138.7 (2C), 138.5, 137.6 (3C), 137.4, 136.9, 136.8, 136.6, 136.3, 136.1, 136.0 (2C), 135.9 (2C), 135.6, 135.4, 135.2, 134.9, 134.8, 134.6, 134.4 (3C), 133.7, 133.6, 133.1, 132.9, 132.3 (2C), 130.2 (Ph), 128.3, 127.9 (Ph), 127.3 (Ph), 57.7 (fullerenyl sp^3 carbon), 46.4 ppm (CH_2). MALDI-TOF MS *m/z*: calcd for $LaC_{89}H_7$ ($[M]^-$), 1213.96; found, 1214.3.

La@C_{82}($CH_2C_6H_5$) (2d). Vis-near-IR (CS_2): λ_{max} = 561, 795, 990, 1274 nm. ^{1}H NMR (500 MHz, CS_2/CD_2Cl_2 = 3/1): δ 7.58−7.50 (m, 2H), 7.39−7.29 (m, 2H), 7.36−7.33 (m, 1H), 4.42 ppm (AB quartet, 2H, Δ_{ab} = 20.0 Hz, J_{ab} = 12.7). ^{13}C NMR (125 MHz, CS_2/CD_2Cl_2 = 3/1): δ 180.1, 170.8, 166.9, 152.3, 151.1, 150.0, 149.8, 149.5, 148.7, 148.3, 148.0, 147.8, 147.7, 147.5, 147.4, 147.4, 147.3, 146.7, 146.6, 146.4, 146.2, 145.8, 145.2, 145.0, 144.7, 144.6, 144.4, 144.3, 144.1, 144.0, 143.9, 143.8, 143.6, 143.4, 142.7, 142.6, 142.4, 142.2, 142.1, 141.8, 141.7, 141.1, 141.0, 140.9, 140.8, 140.5, 140.0, 139.6, 139.4, 139.3, 139.1, 138.6, 138.4, 138.3, 138.1, 138.0, 137.7, 137.5, 137.2, 137.1, 136.5, 136.1 (2C), 136.0, 135.8, 135.7, 135.6, 135.3, 134.8, 134.6, 134.2, 134.0, 133.9, 133.6, 133.4, 133.1, 131.9, 131.6, 131.5, 131.3, 130.5, 129.8 (2C), 128.9, 128.4, 64.7 (fullerenyl sp^3 carbon), 50.6 ppm (CH_2). MALDI-TOF MS *m/z*: calcd for $LaC_{89}H_7$ ($[M]^-$), 1213.96; found, 1214.5.

Radical Reaction of La@C_{82} in Various Solvents by Photoirradiation. A 2.0 × 10^{-1} mL aliquot of a 1.0 × 10^{-4} M La@C_{82} (2.2 × 10^{-2} mg, 2.0 × 10^{-8} mol) solution was placed in a quartz tube. *p*-Xylene, *o*-xylene, *p*-*tert*-butyltoluene, and α,α,2,4-tetrachlorotoluene (**4**) were used as solvents. Then the solution was degassed by freeze−pump−thaw cycles under reduced pressures and irradiated by a high-pressure mercury-arc lamp (cutoff <330 nm). The reaction mixture was injected into an HPLC for analysis and subjected to MALDI TOF mass analysis.

Synthesis of La@C_{82}($CHClC_6H_3Cl_2$) (3). 4 (6.9 mL, 9.7 mg, 4.2 × 10^{-7} mol) was added to 40 mL of 1.5 × 10^{-4} M La@C_{82} (6.7 mg, 6.0 × 10^{-6} mol) ODCB solution. Then the solution was placed in a Pyrex tube, degassed by freeze−pump−thaw cycles under reduced pressures, and then irradiated by a high-pressure mercury-arc lamp (cutoff <330 nm) for 3 min. The two isomers (**3b** and **3d**) were successfully isolated from the other isomers and unreacted starting materials by the multistep preparative HPLC procedure (Figure S12).

La@C_{82}($CHClC_6H_3Cl_2$) (3b). Vis-near-IR (CS_2): λ_{max} = 566, 770, 1154, 1299 nm. ^{13}C NMR (125 MHz, CS_2/CD_2Cl_2 = 3/1): δ 178.6, 169.6, 166.3, 163.8, 160.3, 151.4, 149.7, 148.8, 148.6, 148.1, 147.8, 147.7, 147.4, 147.3, 146.9, 146.8, 146.3, 146.0, 145.9, 145.8, 145.7, 145.6, 145.1, 144.6, 144.4, 144.1, 143.9, 143.9, 143.5, 143.0, 142.3 (2C), 142.0, 141.9 (2C), 141.8, 141.6, 141.5, 141.4, 141.2, 140.9, 140.6, 139.8, 139.7, 139.4, 139.2, 139.1, 138.9, 138.8, 138.3, 137.9, 137.5, 137.3, 137.1, 137.0, 136.6, 136.6, 136.5, 136.1, 135.9 (2C), 135.8, 135.7, 135.6, 135.5, 135.0, 134.6, 134.1, 134.0, 133.9, 133.6 (2C), 133.5, 133.3, 133.0 (2C), 132.4, 132.3, 132.1, 129.6, 129.2, 128.9, 128.8, 128.0, 127.9, 125.1, 124.5, 67.1, 64.5 ppm. MALDI-TOF MS *m/z*: Calcd for $LaC_{89}H_4Cl_2$ ($[M - Cl]^-$), 1280.88; $LaC_{89}H_4Cl$ ($[M - 2Cl]^-$), 1245.91. Found, 1281.1; 1246.1.

La@C_{82}($CHClC_6H_3Cl_2$) (3d). Vis-near-IR (CS_2): λ_{max} = 556, 785, 1004, 1280 nm. ^{13}C NMR (125 MHz, CS_2/CD_2Cl_2 = 3/1): δ 175.3, 166.0, 161.2, 151.7, 150.0, 149.8, 149.0, 148.9, 147.4, 147.4, 147.0, 147.0, 146.9, 146.9, 146.6, 146.5, 145.8, 145.5, 145.3, 145.2, 145.1, 144.7, 144.4, 144.0, 143.4, 143.3, 143.1 (2C), 143.0, 141.8 (2C), 141.7 (2C), 141.3, 141.2, 140.8, 140.7, 140.4, 140.1, 139.9 (2C), 139.5, 138.8, 138.4, 137.9 (2C), 137.7, 137.2 (2C), 137.1, 137.1, 137.0 (2C), 136.8, 136.6, 136.4, 136.4, 136.0, 135.3, 135.1, 135.0, 134.9, 134.7, 134.6, 134.5, 134.2, 134.0, 133.5, 133.0, 132.8, 132.6, 132.4, 132.3 (2C), 132.2 (2C), 131.6, 131.1, 130.3, 129.2, 129.0, 128.4, 128.1, 127.4, 127.2, 126.9, 125.1, 66.4, 64.8 ppm. MALDI-TOF MS *m/z*: Calcd for $LaC_{89}H_4Cl_2$ ($[M - Cl]^-$), 1280.88; $LaC_{89}H_4Cl$ ($[M - 2Cl]^-$), 1245.91. Found, 1281.3; 1246.2.

Black crystals of **3d**·1(CS_2) were obtained by liquid−liquid bilayer diffusion methods of a solution of **3d** in CS_2 and hexane used as a poor solvent. Single-crystal XRD data were collected at beamline BL-1B of the Photon Factory, KEK, Japan, in the scan range −90.0° < θ < 90.0°. Crystal data of **3d**·1(CS_2): $C_{90}H_4Cl_3S_2La$, M_W = 1394.31, monoclinic, space group *P21/n*, *a*

Scheme 1

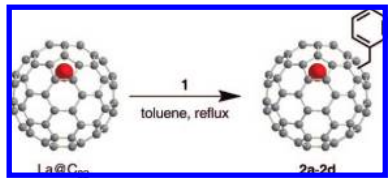

= 11.276(6) Å, b = 21.827(13) Å, c = 19.094(11) Å, $\alpha = \beta$ = 90.00°, γ = 90.72(15)°, V = 4699.0(5) Å^3, Z = 4, D_{calc} = 1.971 Mg/m^3, μ = 1.237 mm^{-1}, T = 130(2) K, crystal size 0.10 × 0.07 × 0.07 mm^3; 22 521 reflections, 11 298 unique reflections; 6135 with $I > 2\sigma(I)$; $R_1 = 0.1235[I > 2\sigma(I)]$, $wR_2 = 0.3617$ (all data), GOF (on F^2) = 1.300. The maximum residual electron density is 1.250 eÅ^{-3}.

Theoretical Calculations. Geometries were optimized using the Gaussian 03 program[19] with density functional theory (DFT) at the B3LYP level[20−23] (ECP[24] and (5s5p3d)/[4s4p3d] for La, and 3-21G for C, H, and Cl,[25] B3LYP/3-21G∼dz for short). Energies were calculated at the B3LYP/6-31G*∼dz//B3LYP/3-21G∼dz level for La@C_{82}($CH_2C_6H_5$) and at the B3LYP/6-31G*∼dz//B3LYP/6-31G*∼dz and MPW1B95/6-311G*∼dz//B3LYP/6-31G*∼dz levels[26] for La@C_{82}($CHClC_6H_3Cl_2$). ^{13}C NMR chemical shifts were calculated at the B3LYP/6-311G*∼dz//B3LYP/3-21G∼dz level.

Reaction of La@C_{82} with 1 in Benzene. 1 (4.4×10^{-1} mg, 1.2×10^{-6} mol) was added to 3 mL of 1.2×10^{-4} M La@C_{82} (5.0×10^{-1} mg, 4.4×10^{-7} mol) in benzene solution. The solution was placed in a Pyrex tube, degassed by freeze−pump−thaw cycles under reduced pressures, and then heated at 380 K for 15 h. Two fractions were isolated from unreacted **1** and La@C_{82} by preparative HPLC using a Buckyprep column. A fraction containing only one of the isomers of La@C_{82}($C_2H_2NCPh_3$) (**5a**) was isolated successfully, and the posterior fraction was obtained as a mixture of several isomers, characterized by ESR measurement and MALDI TOF mass analysis (Figures S19−21).

La@C_{82}($C_2H_4NCPh_3$) (5a). MALDI-TOF MS *m*/*z*: calcd for $LaC_{103}H_{17}N$ ($[M]^+$), 1407.05; found 1408.2. ESR: *hfcc* = 1.20 Gauss, *g*-value = 2.0017.

Tracing EPR Measurements of the Thermal Reactions of La@C_{82} with 1. To a 0.20 mL aliquot of 5.0×10^{-4} M La@C_{82} (1.1×10^{-2} mg, 1.0×10^{-8} mol) solution of toluene or benzene, **1** (1.8×10^{-2} mg, 5.0×10^{-8} mol) was added respectively. The solutions were placed in quartz tubes individually, degassed by three freeze−pump−thaw cycles under reduced pressures, and then heated at 388 K. EPR signal intensities were recorded in integrated EPR spectra with Gaussian function fitting.

Results and Discussion

Formation, Isolation, and Characterization of Benzyl Adducts (2a−2d). A toluene solution of La@C_{82} in the presence of **1** was refluxed to afford **2a**−**2d** (Scheme 1). This result indicates that the formation of **2a**−**2d** is caused by the direct addition of the benzyl radical, produced in situ by hydrogen abstraction from toluene in the presence of **1**, to La@C_{82}. In this context, the azomethine ylide intermediate may play an important role to generate the benzyl radical.

The HPLC isolation procedures are illustrated in Figure 1. Two monoadducts (**2a** and **2d**) were isolated by a two-step HPLC method, and two more regioisomers (**2b** and **2c**) were obtained after a three-step HPLC separation. The insets of Figure 2 and the Supporting Information show HPLC profiles of the purified samples. The product distribution was estimated to be approximately 18% for **2a**, 34% for **2b**, 22% for **2c**, and 26% for **2d** according to the analyses of their HPLC profiles.

The magnetic properties of **2a**−**2d** were studied by ESR spectroscopy (not shown). All these monoadducts were found to be ESR-inactive because of the coupling of La@C_{82} and benzyl radicals.

The MALDI-TOF mass spectra of **2a**−**2d** are depicted in Figure 2. Similar mass spectra were observed in both positive and negative modes. The peak at *m*/*z* 1214 is attributed to the benzyl monoadduct of La@C_{82}. On the other hand, peaks at *m*/*z* 1123 and 1305 correspond to the fragments formed by the loss and intermolecular transfer of the benzyl group, respectively, which are caused by the laser desorption process in the observation of mass spectra.

Figure 3 shows the absorption spectra of **2a**−**2d**. These absorption spectra are considerably different from that of La@C_{82}. Their characteristic absorption onsets move to shorter wavelengths (ca. 1600 nm) than that of La@C_{82}, indicating that **2a**−**2d** have larger HOMO−LUMO energy gaps due to the closed shell structures. The absorption spectra of fullerene derivatives in near-IR field are believed to be independent of the nature of addends. We have recently determined the addition site of a Bingel adduct of La@C_{82}, La@$C_{82}CBr(CO_2C_2H_5)_2$ (**6**) (denoted as "mono-A" in ref 11a), by XRD analysis. The similarity in the absorption of **6** and **2a** indicates that these two monoadducts have the same addition site.

As Figure 4a shows, the ^{1}H NMR spectrum of **2b** exhibits clearly the spectral pattern of its benzyl group. The aromatic protons of the benzyl group are observed in the region between 7.4 and 7.8 ppm. The signals at 4.77 and 4.88 ppm are assignable to the AB quartet by diastereotopic geminal protons in the methylene group. The ^{13}C NMR spectrum of **2b** in Figure 4b shows a total of 87 lines. This indicates that **2b** has C_1 symmetry, because the 87 lines are assigned to nonequivalent 82 lines from the C_{82} cage and 5 lines from the benzyl group by ^{1}H−^{13}C long-range coupling NMR measurements (Figures S3 and S4). The signal at 62.2 ppm is assigned to the sp^3 carbon atom on C_{82}, and the signal at 47.7 ppm is due to the methylene carbon atom. The marked signals in the low magnetic field are attributed to the carbon atoms adjacent to the sp^3 carbon atom on C_{82}. ^{1}H NMR and ^{13}C NMR spectra of **2c** and **2d** were also recorded, indicating that they also have C_1 symmetry (Figures S5 and S6).

Radical Reaction upon Photoirradiation. We found that a solution of La@C_{82} and toluene affords benzyl radical adducts only upon photoirradiation, without the existence of **1**. When the solution, degassed by three freeze−pump−thaw cycles, in a sealed quartz tube was photoirradiated by a high-pressure mercury-arc lamp (cutoff <330 nm) for 5 s, the formation of benzyl adducts was observed from HPLC and MALDI-TOF analysis (Figure S7). Interestingly, photoirradiation by sunlight for 1 h also gave the benzyl adducts (Figures S8 and S9). From these results, we speculate that a trace of oxygen in toluene is sufficient to trigger the radical reaction.

(19) Frisch, M. J. et al. *GAUSSIAN 03*, revision C.01; Gaussian Inc.: Wallingford, CT, 2004.
(20) Becke, A. D. *Phys. Rev. A* **1988**, *38*, 3098–3100.
(21) Becke, A. D. *J. Chem. Phys.* **1993**, *98*, 5648–5652.
(22) Lee, C.; Yang, W.; Parr, R. G. *Phys. Rev. B* **1988**, *37*, 785–789.
(23) Francl, M. M.; Pietro, W. J.; Hehre, W. J.; Binkley, J. S.; Gordon, M. S.; DeFrees, D. J.; Pople, J. A. *J. Chem. Phys.* **1982**, *77*, 3654–3665.
(24) Hay, P. J.; Wadt, W. R. *J. Chem. Phys.* **1985**, *82*, 299–310.
(25) Binkley, J. S.; Pople, J. A.; Hehre, W. J. *J. Am. Chem. Soc.* **1980**, *102*, 939–947.
(26) Zhao, Y.; Truhlar, D. G. *J. Phys. Chem. A* **2004**, *108*, 6908–6918.

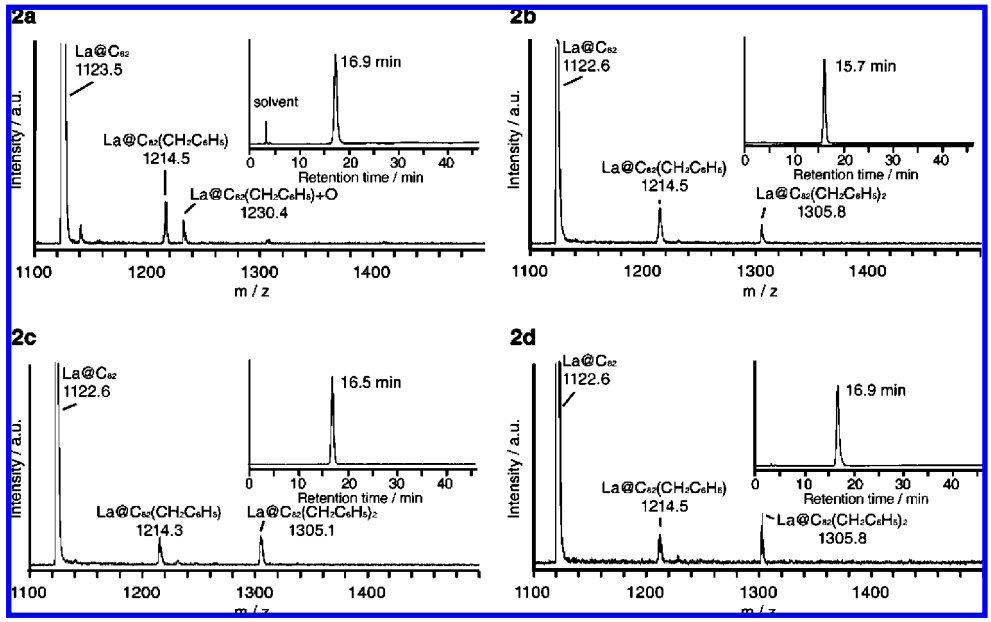

Figure 2. MALDI TOF-mass spectra of **2a**, **2b**, **2c**, and **2d**. The insets show the HPLC profiles. Conditions: column, Buckyprep (i.d. 4.6 mm × 250 mm); eluent, toluene; flow rate, 1.0 mL/min; wavelength, 330 nm; room temperature.

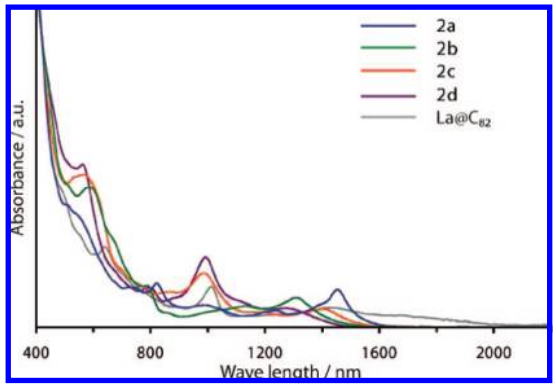

Figure 3. Vis-near-IR absorption spectra of **2a**−**2d** and La@C_{82} in CS_2.

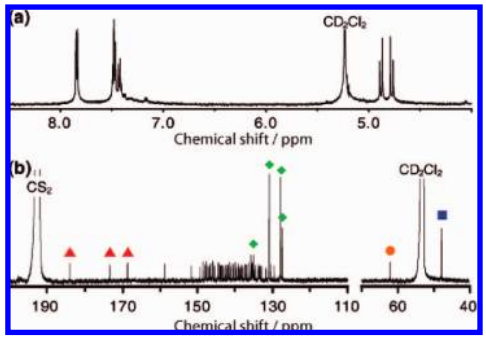

Figure 4. (a) ^{1}H NMR and (b) ^{13}C NMR spectra of **2b** in CS_2/CD_2Cl_2 = 3/1 (v/v). Orange, red, blue, and green solid symbols are due to the sp^3 carbon atom of the addition site, the sp^2 carbon atoms next to the addition site, the methylene carbon of the benzyl group, and the other carbon atoms of the benzyl group, respectively.

Similar reactions were also observed for other paramagnetic EMFs such as La@$C_{82}(C_s)$ and Ce@$C_{82}(C_{2v})$ (Figure S10). However, the reactions were not observed for diamagnetic La_2@$C_{80}(I_h)$. These suggest the characteristic behavior of toluene to paramagnetic EMFs. In this context, it is interesting that a series of substituted benzenes, such as *p*-xylene, *o*-xylene, *p*-*tert*-butyltoluene, and **4**, can be alternatives to toluene, affording the corresponding derivatives (Figure S11).

Scheme 2

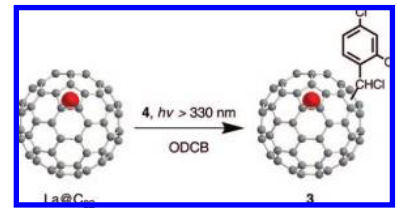

Formation and Characterization of La@C_{82}($CHClC_6H_3Cl_2$) (3). These derivatives **3**were synthesized by the photochemical reaction of La@C_{82} with **4** in ODCB (Scheme 2). Eight isomers were observed at least, and the two isomers (**3b** and **3d**) were isolated successfully by multistep HPLC (Figure S12). Since **3b** and **3d** are silent in ESR spectroscopy, they have a closed-shell structure. As Figure 5 shows, **3b** resembles **2b** in the absorption spectrum, while **3d** resembles **2d**. This suggests that the addition position is the same for **3b** and **2b** as well as **3d** and **2d**. The ^{13}C NMR spectra of **3b** and **3d** show a total of 89 lines (82 lines from the carbon cage and 7 lines from the trichlorobenzyl group), indicating that they have C_1 symmetry (Figure S17a, b).

X-ray Crystallography of 3d. We succeeded in obtaining single crystals of **3d** suitable for XRD measurement. The structure of **3d** was determined by X-ray crystallographic analysis at 130 K. As shown in Figure 6, the trichlorobenzyl group is linked to the fullerene cage by forming one carbon−carbon single bond. Notably, the addition site is near the equator of La@C_{82}, which is very distinct from those of the monoaddition derivatives of M@C_{82} reported previously.[13a,c,14a,15h] To the best of our knowledge, **3d** is the first example of addition to a carbon near the equator of M@C_{82}.

Theoretical Calculations. We have calculated the ^{13}C NMR chemical shifts of **3d** in the DFT optimized X-ray crystal structure. The calculated NMR pattern is in good agreement with the observed one (Figure S17c).

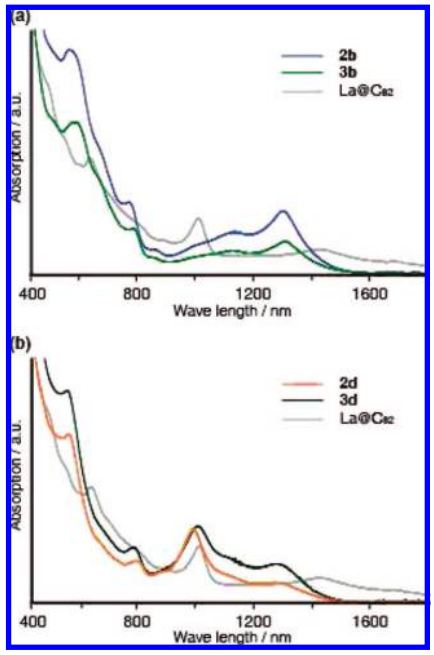

Figure 5. Vis-near-IR absorption spectra of (a) **2b** and **3b** and (b) **2d** and **3d**, in toluene.

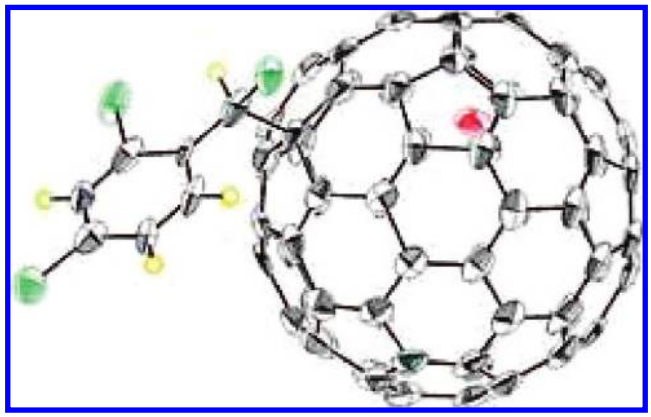

Figure 6. ORTEP drawing of **3d** in 50% probabilities. CS_2 is omitted for clarity.

Table 1. Spin Densities and POAV Values of the Carbon Atoms in La@C_{82}, and the Relative Energies (kcal/mol) of the Isomers of **2** and **3** Calculated at the B3LYP Level

carbon number	spin density	POAV value	rel energies of the isomers of **2**	rel energies of the isomers of **3**[a]
C2	0.022	11.28	0.0	0.0 (0.0)
C23	0.062	10.74	1.33	2.87 (3.43)
C14	0.057	11.01	1.60	3.11 (3.74)
C10	0.066	10.66	1.78	3.45 (3.77)
C18	0.045	11.01	1.65	3.74 (4.36)
C1	−0.012	11.20	8.28	

[a] Values in parentheses are calculated at the MPW1B95 level.

The spin densities were computed at the B3LYP/3-21G∼dz level within the Mulliken population analysis. The calculated spin densities and the p-orbital axis vector (POAV) of the carbon atoms ($\theta\Delta\pi$-90°) in La@C_{82} are given in Table 1.[27] As shown in Figures 6 and 7, C10 is the addition site of **3d** (**2d**) determined by XRD analysis and C23 is the addition site of **2a** expected

(27) Haddon, R. C. *Science* **1993**, *261*, 1545–1550.

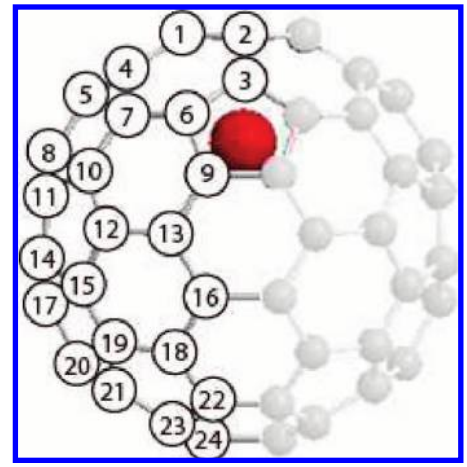

Figure 7. Schematic drawing of La@$C_{82}(C_{2v})$.

Table 2. Redox Potentials[a,b]

compound	E_{ox}^1	E_{red}^1	E_{red}^2	E_{red}^3
2a	0.25	−0.68	−1.02	−1.21
2b	0.21	−0.95	−1.40	
2c	0.17	−0.84	−1.42	−1.74
2d	0.15	−1.05	−1.15	−1.81
3b	0.24	−0.91[c]	−1.39[c]	
3d	0.25	−0.98[c]	−1.07[c]	−1.34[c]
6[d]	0.38	−0.66	−1.31	−1.47
7[e]	0.01	−0.49	−1.44	−1.79
La@$C_{82}(C_{2v})$[f]	0.07	−0.42	−1.37	−1.53

[a] Values in volts relative to a ferrocene/ferrocenium redox couple are obtained by DPV. [b] Conditions: working electrode and counter electrode, platinum wire; reference electrode, SCE; supporting electrolyte, 0.1 M (nBu)$_4$NPF$_6$ in ODCB. CV: scan rate, 50 mV s^{-1}. DPV: pulse amplitude, 50 mV; scan rate, 20 mV s^{-1}. [c] Irreversible. [d] Reference 13a [e] Reference 14a [f] Reference 6b.

from the similarity in absorption spectra between **2a** and **6**. It is interesting that the C10 and C23 atoms have larger spin densities than other carbons of La@C_{82}. Since C14 and C18 have relative large spin densities and POAV values, these are the probable addition sites of **2b** (**3b**) and **2c**.

The isomers of **2** and **3** were optimized, which have addition sites at C1, C2, C10, C14, C18, and C23. The calculated relative energies at the B3LYP level are also given in Table 1. The isomer with the addition site at C2 is the most stable for both **2** and **3**. However, this isomer of C_s symmetry can be excluded, because ^{13}C NMR indicates C_1 symmetry. In addition, the relative energies in Table 1 do not agree well with the experimental results. This trend is also true at the MPW1B95 level (see Table 1). These suggest that the addition sites are not thermodynamically but kinetically controlled. In this context, spin densities are more helpful to predict the addition sites.

Electrochemical Properties. Table 2 shows the redox potentials of **2a**−**2d**, **3b**, **3d**, **6**,[13a] La@C_{82}Ad (**7**; Ad = adamantylidene),[14a] and La@C_{82}[6a] obtained by DPV. The salient features of **2a**−**2d**, **3b**, **3d**, and **6** are the wider gap between their first redox potentials. It is interesting that the first redox potentials of singly bonded derivatives of La@C_{82} do not depend on the difference between addition positions. On the other hand, the second and third reduction potentials are affected by the addition sites. As a result, **2b** and **3b** as well as **2d** and **3d** have similar redox potentials, since each pair has the same addition site. The CV study shows that **2a**−**2d** exhibit four reversible

Scheme 3

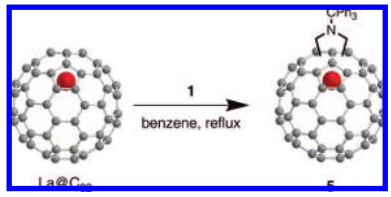

waves, while the first reduction of **3b** and **3d** is irreversible (Figure S18). This suggests that the anions of **3b** and **3d** are unstable.

Metallofulleropyrrolidine, La@C_{82}($C_2H_4NCPh_3$). The thermal reaction of La@C_{82} and **1** in benzene provides metallofulleropyrrolidine derivatives La@C_{82}($C_2H_4NCPh_3$) (**5**) as major products, unlike the reaction in toluene leading to **2a**−**2d** (Scheme 3). One of the isomers, **5a**, is successfully isolated by HPLC and confirmed by ESR and MALDI-TOF mass spectra, as shown in the Supporting Information. Since it is well-known that thermal reactions of oxazolidinones produce reactive azomethine ylides, oxazolidinones are often used to prepare various functionalized fulleropyrrolidines.[12,28] We recently reported the synthesis and characterization of the metallofulleropyrrolidine derivative La_2@C_{80}(I_h)($C_2H_4NCPh_3$) by the thermal reaction of La_2@C_{80}(I_h) with **1** in toluene.[12e] In contrast, the reaction of La@C_{82} and **1** in toluene indicates that the addition of the benzyl radical to La@C_{82} is more preferable than the direct addition of the azomethine ylide.

Tracing EPR of the Thermal Reactions of La@C_{82} with 1. In-situ EPR measurement of the thermal reaction of La@C_{82} with **1** revealed the different behavior between the formation of **2a**−**2d** and **5**. The EPR intensity of La@C_{82} decreased rapidly in a few hours in toluene; meanwhile, the intensity decreased much slowly in benzene under the same conditions (Figure 8). The half-life of the La@C_{82} in benzene is ca. 13.0 h, which is 4.4 times longer than that in toluene (ca. 3.0 h) (see Figure S23). This result suggests that the addition of benzyl radical is more favorable than that of the azomethine ylide. In addition, some new signals from products were detected in benzene solution, as shown in Figure 8b, indicating the doubly bonded addition of the azomethine ylide to La@C_{82}. In contrast, any of the new signals were not detected in toluene, suggesting that stable compounds which have an even number of addends were not formed in situ during the heating period.

Conclusion

The addition reaction of radical groups to La@C_{82} leads to stable and novel derivatives in a selective way. The reaction is triggered by initiators, such as oxazolidinone or oxygen. A series of substituted benzenes can be used as a precursor of the radical addition reaction, even though benzene is not reactive to La@C_{82}. Monoadducts **2a**−**2d**, **3b**, and **3d**, which result from radical coupling, have a closed-shell electronic structure. The structure of **3d** is determined by XRD crystallography. Radical coupling reactions take place at the cage carbons that have high spin densities. It is expected that the selective radical reactions of paramagnetic EMFs will open a new methodology in preparing functionalized metallofullerenes.

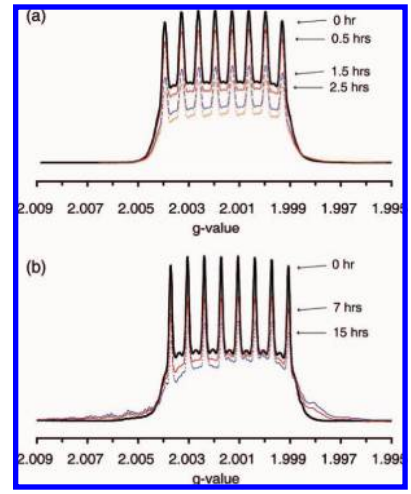

Figure 8. Integrated tracing EPR spectra of the thermal reactions of La@C_{82} with **1** (a) in toluene and (b) in benzene, recorded under the same conditions but with different heating times. Some new peaks appeared under the conditions in benzene after heating.

Acknowledgment. We thank H. Sawa for his experimental help at the Photon Factory. H.N. and M.Y. thank the Japan Society for the Promotion of Science (JSPS) for the Research Fellowship for Young Scientists. This work was supported in part by a Grant-in-Aid, the 21st Century COE Program, Nanotechnology Support Project, The Next Generation Super Computing Project (Nanoscience Project), and Scientific Research on Priority Area from the Ministry of Education, Culture, Sports, Science, and Technology of Japan, and a grant from the Kurata Memorial Hitachi Science and Technology Foundation.

Supporting Information Available: Crystallographic data in CIF format of **3d**, the complete list of authors for refs 51, 19, and 19, spectroscopic data for **2a**−**d**, **3b**, **3d**, and **5a**, separation procedure of **3** and **5**, and Cartesian coordinates (Å) of the C1, C2, C10, C14, C18, and C23 adducts. This material is available free of charge via the Internet at http://pubs.acs.org.

JA802748Q

(28) Prato, M.; Maggini, M. *Acc. Chem. Res.* **1998**, *31*, 519–526.